

Effect of metal doping on the physical properties of TiO_2 nano particle prepared by eco - friendly method

Heba S.Mahfouz¹, Islam M.Moustafa¹, Eman A.Mohamed² and S. M.Mabrouk¹

Chemistry Dept., Faculty of Science, Benha University, Benha, Egypt.¹

International Academy for Engineering and Media Science (IAEMS)²

E-mail: hebasamer683@gmail.com

Abstract

In this work, titanium tetraisopropoxide (at 5.0 mM concentration) was used as a precursor and pomegranate peel extract was used as a bio-reductant to successfully synthesize TiO_2 and metal ion-doped TiO_2 Nanoparticles ($M = \text{Fe}, \text{Cu}, \text{Zn}, \text{and Zr}$) via the green route using the co-precipitation technique. Using a variety of methods, the produced Nanoparticles were described (EDX, XRD, FTIR and TEM). The primary objective is to investigate how the doping cation affects titanium dioxide's structural and photocatalytic characteristics. The various doping Nanoparticles were contrasted in an effort to increase titanium dioxide's photocatalytic activity. The XRD results demonstrated that all of the metal ions were either positioned at the interstitial site or integrated into the structures of titania, and that doping the metal ions in the crystal lattice did not alter the high crystallinity of the TiO_2 structure. It was discovered that the doping process improves the catalytic activity of TiO_2 NP by lowering its gap energy from 3.53 eV in TiO_2 NP to 1.61, 1.65, and 1.8 eV for Fe, Cu, and Zr doped NP, respectively, allowing its use in the visible rather than the ultraviolet region of light. The main goal of the study is to examine the effect of the doping cation on the structural and photocatalytic properties of titanium dioxide.

Key words: doping TiO_2 Nano particles, green chemistry, pomegranate peel extract.

Introduction

Nanotechnology deals with improving the physical and chemical parameters of Nano materials that enhances their use in various purposes specially in the field of catalysis. Due to its large band gap, TiO_2 NP is a semiconductor with low photocatalytic efficiency in visible light [1]. However, doping is known to boost the semiconductor's photocatalytic activity when exposed to visible light. The type of dopant ion has an impact on TiO_2 's structural characteristics and catalytic activity. Different components, including metals and non-metals, were added to TiO_2 [2, 3]. The most effective are transition elements (TE) ions [4–8], whose incorporation into the titanium dioxide lattice causes the development of new energy levels close to the conduction band. These elements contain partially filled d-orbitals. In addition, using such TE is a less expensive and more inexpensive substitute for elements such noble metals (gold, silver, and platinum group metals) [9–13]. While there are numerous physical and chemical techniques for creating Nanoparticles, the usage of environmentally benign and sustainable plant-based technologies has grown. Plants are advantageous because their synthesis process is aided by capping,

stabilizing, reducing, and oxidative agents. *Punica granatum*, or pomegranate, is one of the most significant plants that belongs to the monogeneric family (Pg). Punicaceae (Pg) and its constituent chemicals exhibit diverse pharmacological and toxicological attributes, such as anti-inflammatory, antioxidant, anti-tumor, and anti-angiogenesis actions [14]. The high nutritious content of pomegranate peel (PP) extract includes antioxidants, phenolics, minerals, and vitamins [15]. In this study, we describe a novel approach to the environmentally friendly, green synthesis of TiO_2 NP, which is also metal-doped with a few transition metals. The main goal of this work is to find out how the doping cation influences the structural and photocatalytic properties of titanium dioxide.

Experimental

Materials and methods

Plant material. The pomegranate fruits were gathered from the neighborhood market in Benha, Egypt, and thoroughly cleaned to get rid of any unnecessary materials. Fruit peels were manually separated from seeds, allowed to dry for three to four days, and then baked for forty-eight hours at seventy degrees Celsius. A hammer mill was then used to finely powder the dried peels [16].



Schem(1)

Preparation of pomegranate peel extract (PPE)

Pomegranate extract was made using the previously mentioned procedure [17], which involved adding roughly 25 grams of dried powder to 1,000 milliliters of 60% ethanol and 1.0 grams of citric acid in a flask. After shaking the mixture for five hours at 400 rpm, filter paper was used to remove the particles. Until it was used, the extract was kept in a screw-cap vial in a dark place at 20°C.

Synthesis of Nano TiO₂

TiO₂ NPs was prepared by the green route using the co-precipitation technique in which titanium tetraisopropoxide (TTIP; AR Grade) whose concentration was maintained at 5.0 mM was used as a precursor and the pomegranate peel extract was used as a bio-reductants. In the procedure, 80 mL of the pomegranate peel extract and 5 mM TTIP solution were combined in a 1:1 (volume/volume) ratio. At room temperature, the mixture was constantly swirled for approximately eight hours at 750 rpm. The white precipitate that formed as a result of Ti⁴⁺'s production serves as evidence for its origin. In order to prevent agglomeration and help the TiO₂ NPs take on the appropriate form and size, the extract from the peel of the *Punica granatum* (pomegranate) serves as a capping and stabilizing agent. To separate the Nanoparticles, the liquid was centrifuged for 10 minutes at 750 rpm after stirring. After six hours of drying at 100°C, the resulting wet powdered TiO₂ NPs were calcined for three hours at 350°C in a muffle furnace.

Synthesis of metal - doped TiO₂

The sol-gel method is the most practical of the various ways to synthesise metal-doped TiO₂, including wet chemical synthesis, hydrothermal, plasma oxidative pyrolysis, and sol-gel [18]. This is due to its simple process, inexpensive cost, high production yield, and low temperature requirements (ambient temperature). M-doped TiO₂ (M = Fe, Cu, Zn, and Zr) was created using combination methods, such as the hydrothermal/sol-gel method. Two milligrams of the prepared Nano

TiO₂ were added to 50–100 milliliters of distilled water in a flask with a flat bottom and a condenser to create a suspended sol. Following that, 50 milliliters of 0.2 M metal salts (Zn (NO₃)₂· 6H₂O, CuCl₂·6H₂O, Fe (NO₃)₃·9H₂O, and ZrOCl₂) were added. The mixture was thoroughly combined and heated, stirring constantly, to 100°C for at least 6 hours. After centrifuging the mixture, the solid and solution were separated. After being cleaned, the obtained sediment was heated for eight hours at 400°C in a muffle furnace.

Characterization of the as-prepared Nano compounds

The as- prepared TiO₂ Nano particles and its Fe, Cu, Zn and Zr doped Nano compounds were characterized as described in our previous work [19] by the following techniques:

i- Fourier transform infrared spectra (FTIR) were recorded using the KBr disk technique on a Nicolet iSio FT-IR spectrophotometer in the 4000–400 cm⁻¹ areas (Chemistry department, Faculty of Science, Benha University, Egypt).

ii- Electronic spectra

Using a Jasco V-530 (UV-Vis) twin beam spectrophotometer (Japan) with a scanning speed of 400 nm/min and a band width of 2.0 nm, electronic spectra were obtained in the solid state (Nujol Mull method) in the 800–200 nm range using a 10 mm matched quartz cell at ambient temperature.

iii- X-ray diffraction

X-ray diffraction analysis (XRD) was performed with an instrument called the SIEMENS D5000. At room temperature, the sample was tested within 2θ of 20° to 80°.

iv- Transmission electron microscopy (TEM) with high resolution

High resolution transmission electron microscopy (HRTEM) was used to examine the morphology and particle shape of the as-prepared samples. A JEOL TEM 2100 high resolution electron microscope operating at 100 kv was used, and the sample was dispersed in ethanol on a copper grid.

v- Dispersive energy X-ray (EDX)

A Horiba EMAX X-act energy dispersive spectroscopy, which was connected to the Hitachi S-4800 system, was used to measure the energy dispersive X-ray spectroscopy (EDX).

Results and discussion

Properties of structure

Here, the energy dispersion X-ray (EDX) spectra, Fourier transform infrared (FTIR) spectroscopy, X-ray diffraction (XRD) patterns, high resolution transmission electron microscopy (TEM), and electronic absorption spectra in the solid-state techniques were used to study the structural properties of pure TiO₂ and those of Fe, Cu, Zn, and Zr-doped TiO₂ Nanoparticles.

EDX stands for energy dispersive X-ray spectroscopy.

Using EDX on the SEM, the elemental analysis of both pure TiO₂ and its metal-doped

Nanoparticles was carried out. Following their mounting on specimen stubs using double-sided tape, the freeze-dried Nanoparticles were coated with gold in a sputter coater, analyzed with a FEG-SEM, and their spherical NPs' EDX spectrum was recorded. Energy/keV and counts/cps were the labels for the x- and y-axes, respectively. As demonstrated in Fig.'s (1a-d), energy dispersive X-ray analysis (EDX) shows a strong signal for the Ti, Fe, Cu, Zn, and Zr, demonstrating the creation of pure and doped Nanoparticles. A semi-quantitative analysis (c. f. Table 1) provided each sample's atomic ratios and component percentage. All four metals were successfully doped, as demonstrated by the EDX analysis, which yielded doping concentrations of 2.3, 11.25, 18.61, and 10.62 percent for Fe, Cu, Zn, and Zr, respectively.

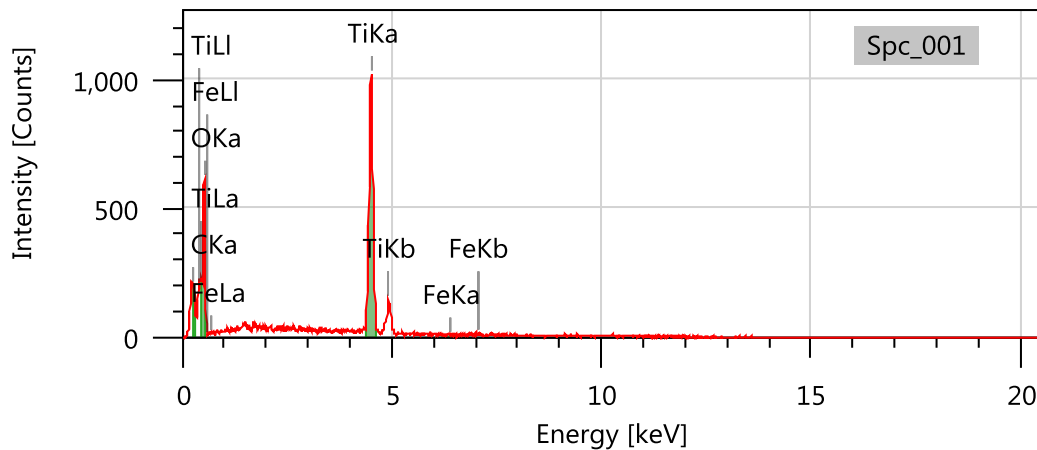


Fig.(1-a): EDX pattern for Fe-TiO₂ doped.

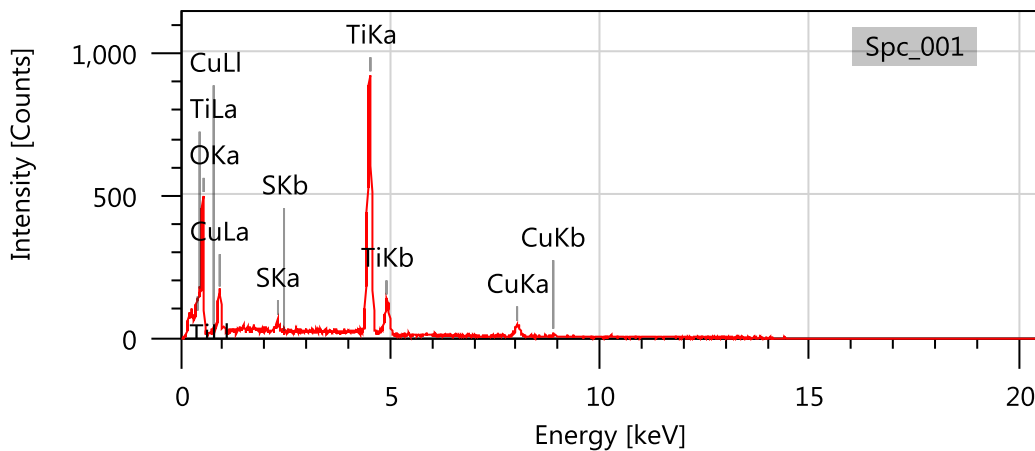


Fig.(1-b): EDX pattern for Cu-TiO₂ doped.

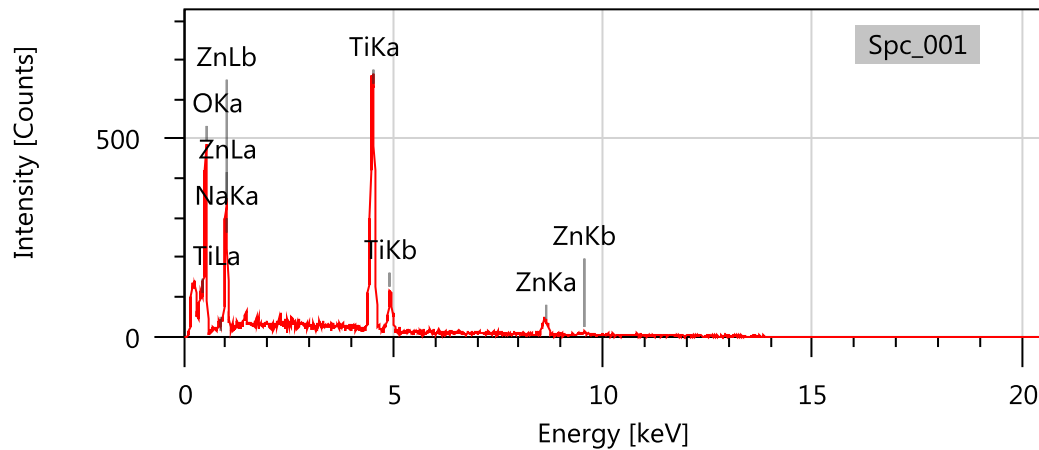


Fig.(1-c): EDX pattern for Zn-TiO₂ doped.

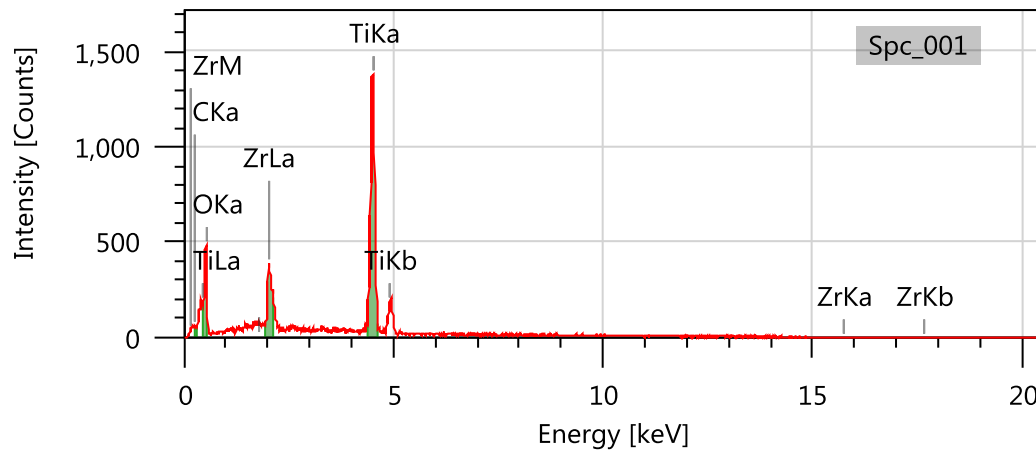


Fig.(1-d): EDX pattern for Zr-TiO₂ doped.

Table (1) Elemental analysis of the as-prepared metal - doped TiO₂ NP gathered from EDX analysis.

Sample	Element	Line	Mass%
TiO ₂ -Fe doped	O	K	51.03±2.25
	Ti	K	47.06±1.41
	Fe	K	0.23±0.17
	Total		100.00
TiO ₂ -Cu doped	O	K	41.86±2.05
	S	K	0.51±0.11
	Ti	K	46.38±1.44
	Cu	K	11.25±1.51
Total		100.00	
TiO ₂ -Zn doped	O	K	39.24±1.96
	Na	K	3.16±0.42
	Ti	K	38.99±1.40
	Zn	K	18.61±2.43
Total		100.00	
TiO ₂ -Zr doped	C	K	Nd
	O	K	35.90±1.82
	Ti	K	53.48±1.32
	Zr	L	10.62±0.53
Total		100.00	

FTIR spectra

. Two different absorption bands were visible in the FTIR spectrum of pure TiO₂, corresponding to stretching TiO, anatase titania, and stretching TiOH, respectively, at 3440 and 1637 cm⁻¹ (Fig. 2). The latter band is explained by the presence of hydrogen (H) impurities in the TiO₂ film, which are covalently bonded to oxygen vacancies and cause n type conductivity in the film [20].

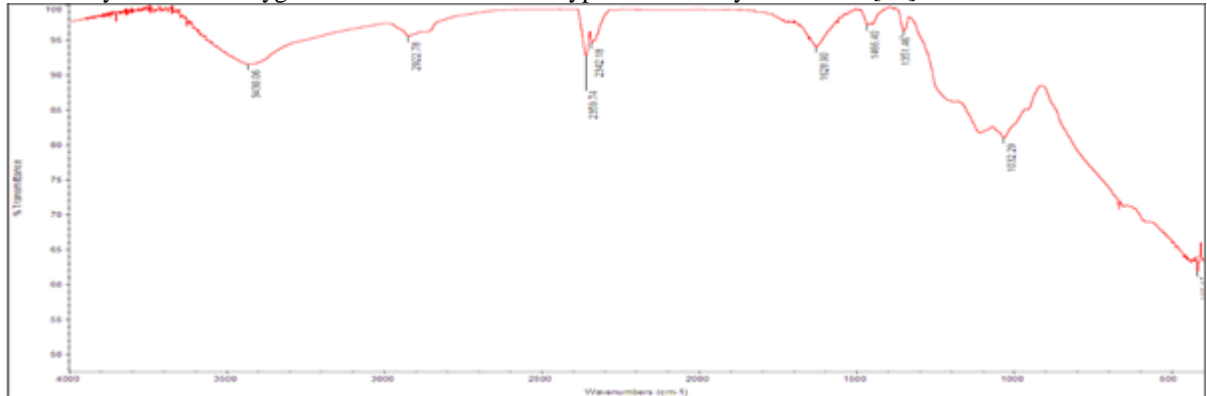


Fig. (2): IR spectrum of TiO₂

However, new absorption bands appeared at 520 cm⁻¹ (Fe-O), 524 cm⁻¹ (Cu-O), 528 cm⁻¹ (Zn-O), and 1108 cm⁻¹ (O-Zr-O) when Fe, Cu, Zn, and Zr metals were added to the TiO₂ Nano particle (c.f. Fig, 3a-d). This confirm the doping formation between these metals and TiO₂ Nano particle the which was previously supported by the data obtained from EDX analysis.

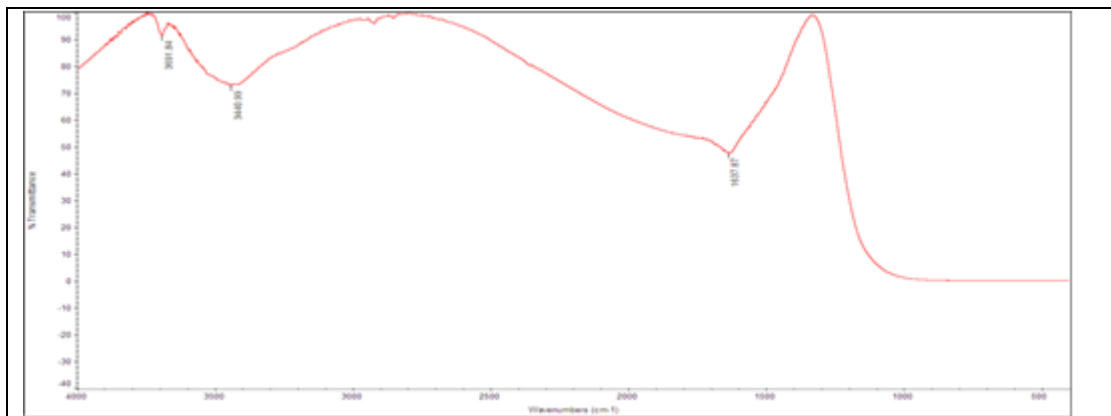


Fig. (2-a): IR spectrum of Fe³⁺-TiO₂ doping.

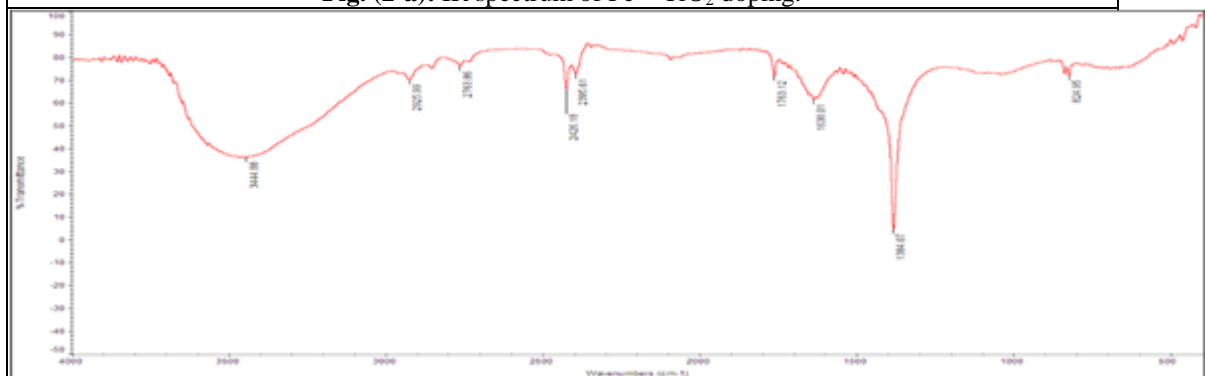


Fig. (2-b): IR spectrum of Cu²⁺-TiO₂ doping.

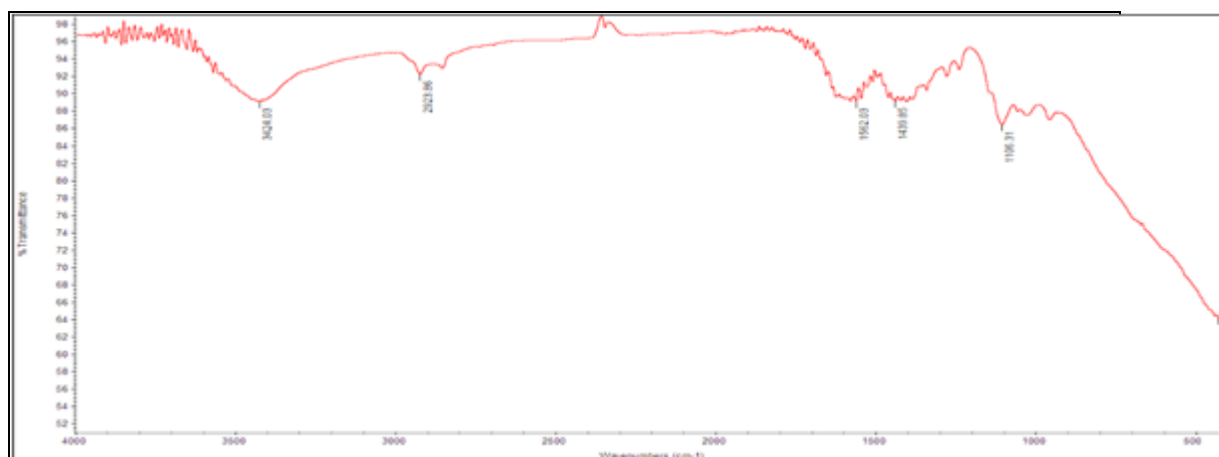


Fig. (2-c): IR spectrum of Zn²⁺-TiO₂ doping.

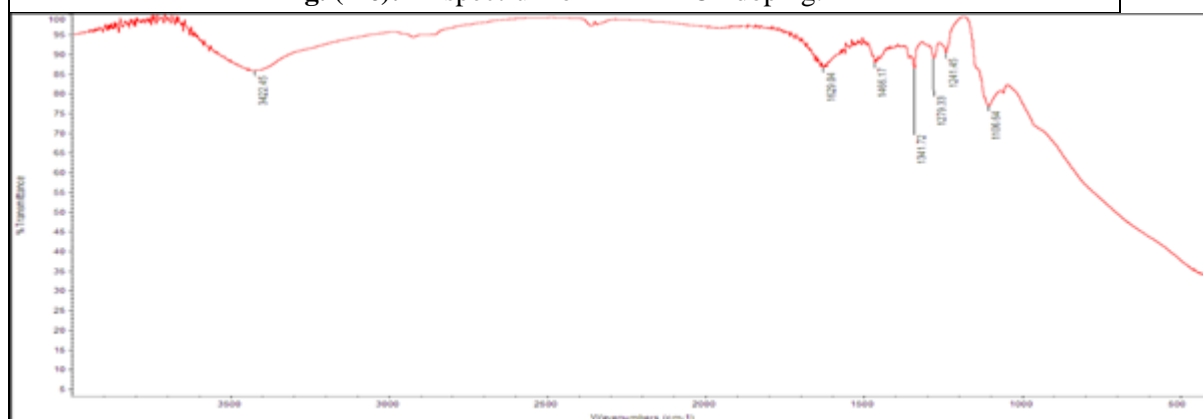


Fig. (2-d): IR spectrum of ZrO₃⁺-TiO₂ doping.

diffraction of X-rays (XRD)

The crystallinity and phase composition of TiO₂-doped with various metals were evaluated by XRD analysis. When Fe, Cu, Zn, and Zr were added to the TiO₂ NP, the crystallinity decreased and new peaks appeared at 2θ of 26.64°, 33.94°, 51.86°, and 57.86°, respectively, indicating the presence of Fe₂O₃, CuO, ZnO, and ZrO₃. Representative example for XRD spectra of Zr-doped TiO₂ Nano particle is shown in Fig. (3).

The Debye-Scherrer equation was used to estimate the average crystal size:

$$D = \frac{k\lambda}{\beta_{hkl}} \cos\theta_{hkl}$$

simplified as: $D = \frac{1}{0.9\lambda\beta} \cos\theta_{hkl}$ [21,22] where, D is the average crystalline size, λ is the wavelength of the X-ray used (λ = 1.5406 Å), β_{hkl} is the FWHM of the diffraction line (in radians), and θ_{hkl} is the Bragg angle corresponding to the diffraction line arising from the planes designated by Miller indices (hkl). The shape factor, k, varies between 0.95 and 1.15 depending on the shape of the grains (k = 0.94 for spherical crystallites). The produced Nanoparticles' estimated average crystal size ranged from 28 to 35 nm based on the X-ray diffraction results.

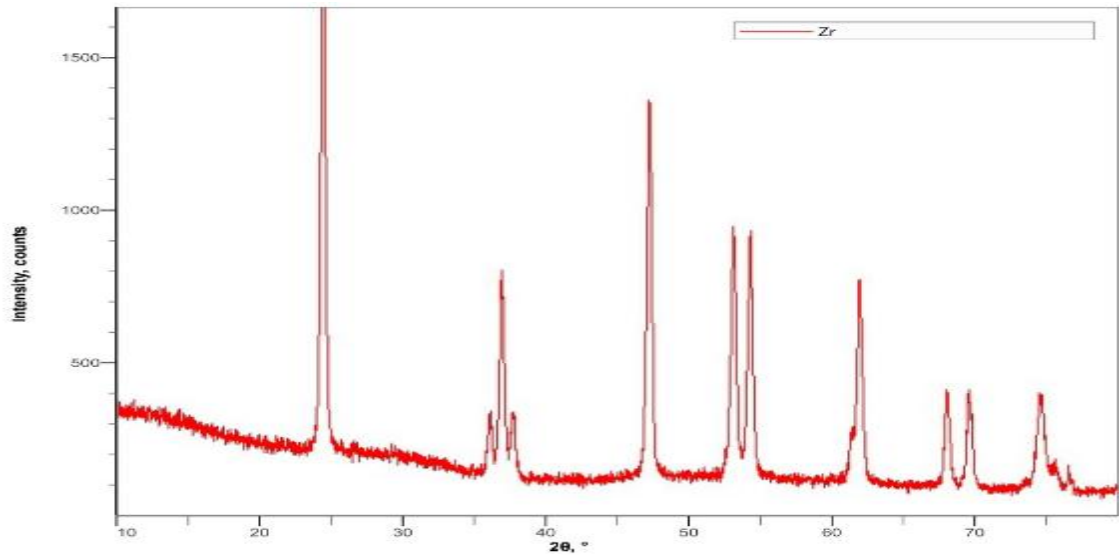


Fig. (3) XRD spectra of Zr-doped TiO₂ Nano particle.

Transmission electron microscopy with high resolution (HRTEM)

Using HRTEM, the micro structural analysis of the as-synthesised samples was examined. It is evident from the TEM pictures taken at various magnification levels (500–5000) that the samples are cube- and spherically-shaped single crystallites, with sizes between 25 and 50 nm. Additionally, the NPs are evenly distributed and have not aggregated, as seen by these photos. In Figs. (4a,b), representative instances are displayed.

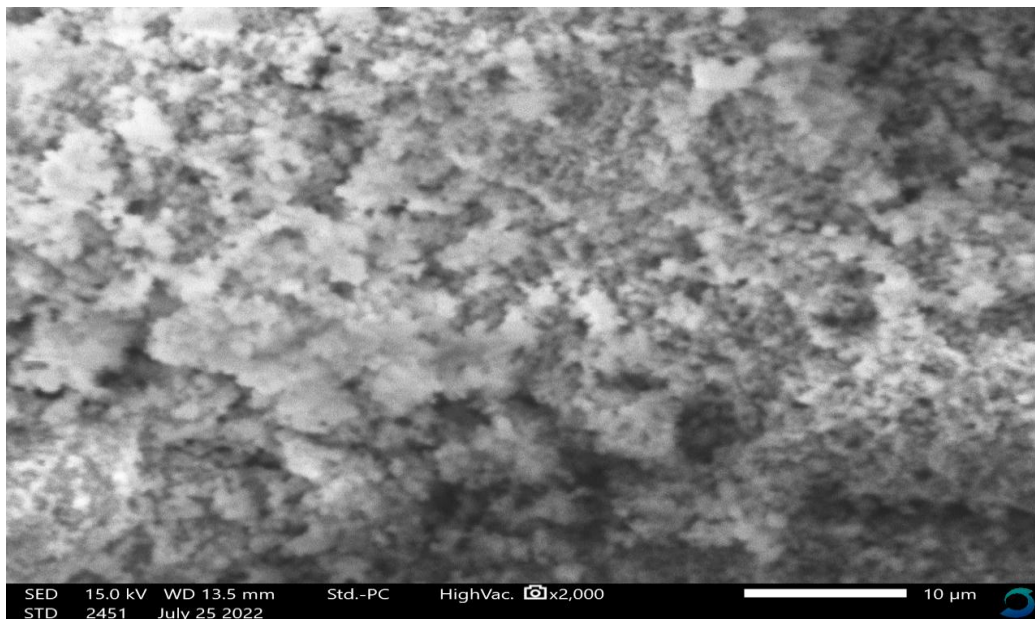


Fig.(4-a) HRTEM images of Zr-doped TiO₂ with 2000 magnification powers

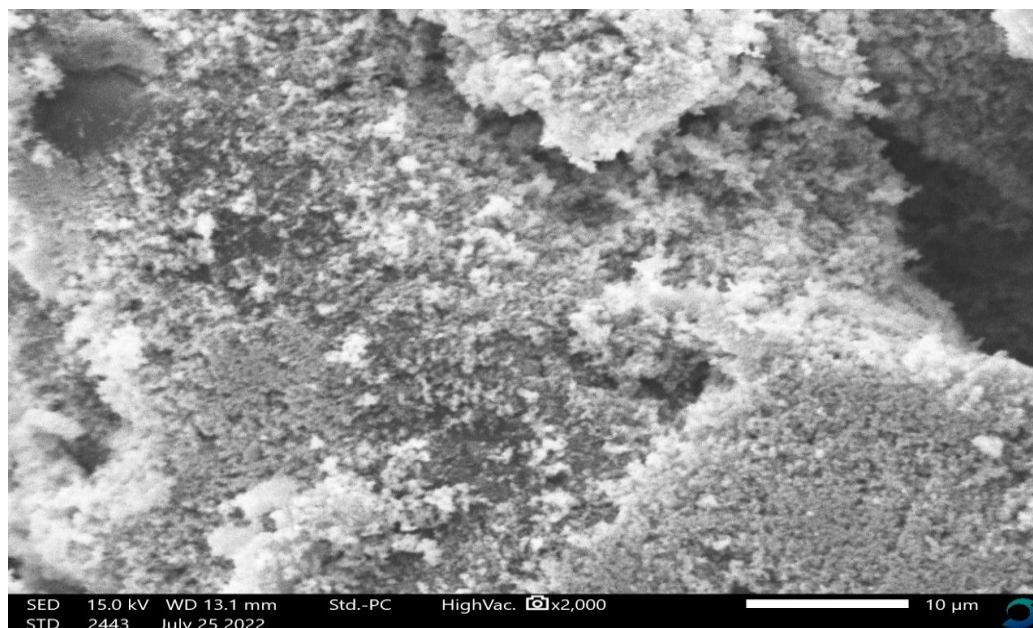


Fig.(4-b) HRTEM images of Fe-doped TiO₂ with 2000 magnification powers

Optical Analysis

The band gap energy is a key characteristic of Nanoparticles. This is the difference in energy between the conduction band, which is empty, and the full valence band. An abrupt rise in absorption at the wavelength corresponding to the band gap energy is produced by significantly permitting optical stimulation of electrons across the band gap. Using the Tauc equation, which represents the relationship between the absorption coefficient (α) and the input photon energy ($h\nu$), one can determine the band gap directly from UV-visible spectra [23].

$$(\alpha h\nu) = A(h\nu - E_g)^n$$

where the exponent n depends on the sort of transition; it can be either 2 for an indirect transition or $1/2$ for a direct transition. E_g is the material's band gap. In this case, the indirect transition indicated by $n = 2$ yields the optimal curve. Plotting the

relationship between $(\alpha h\nu)^2$ vs $h\nu$ and extrapolating the straight-line portion to the $h\nu$ axis allowed for the calculation of the optical band gaps for both pure TiO₂ and its Fe, Cu, Zn, and Zr doped NP. Figures (5a-d) display representative examples of the Tauc plots and the UV-Visible spectra of the investigated Nanoparticles in the solid state (using the Nujol-Mull technique). The energy gaps for TiO₂ and its Fe, Cu, and Zr doped NP are 3.53, 1.61, 1.65, and 1.8 eV, respectively, when the linear component is extrapolated to the $h\nu$ axis. Calculations of E_g values showed that it decreases from 3.53 eV in TiO₂ NP to 1.61, 1.65 and 1.8 eV for Fe, Cu and Zr doped NP, respectively. Thus, the doping process leads to an improvement in the catalytic activity of TiO₂ NP by decreasing its gap energy allowing its use in the visible region of light rather than in the ultraviolet region.

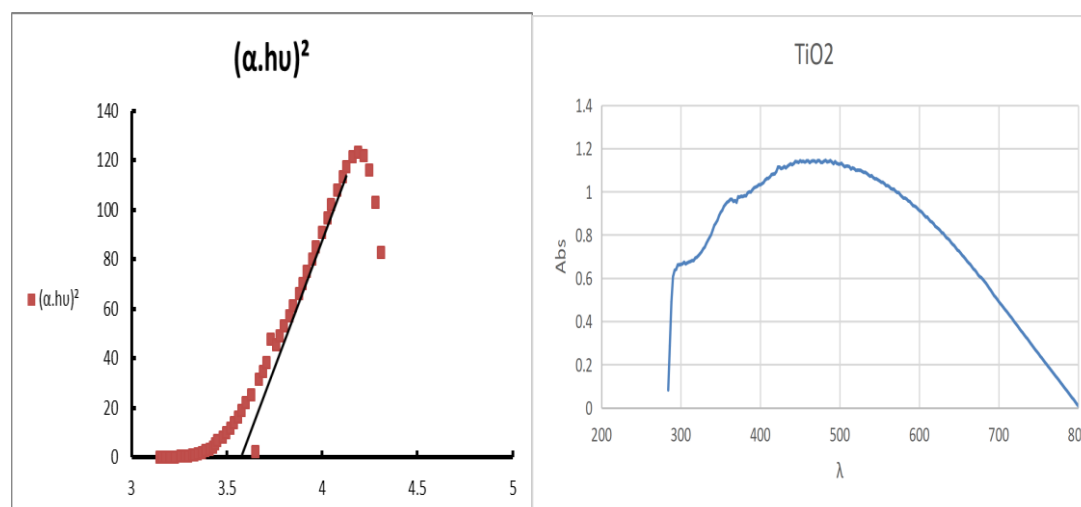


Fig.(5a) Electronic absorption spectrum of TiO₂ NP in nujol mull and Tauc plot of $(\alpha h\nu)^2$

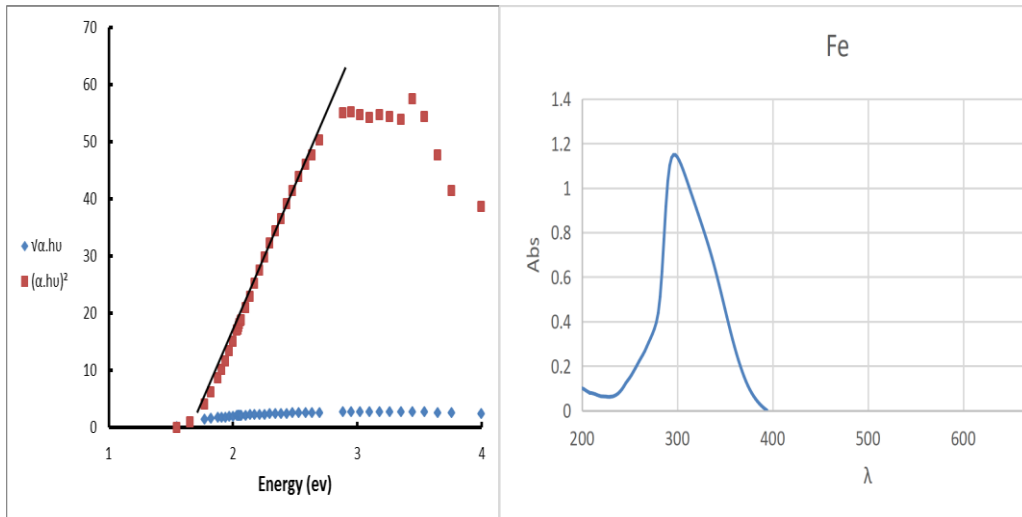


Fig.(5b) Electronic absorption spectrum of doped Fe-TiO₂ NP in nujol mull and Tauc plot of $(\alpha h\nu)^2$

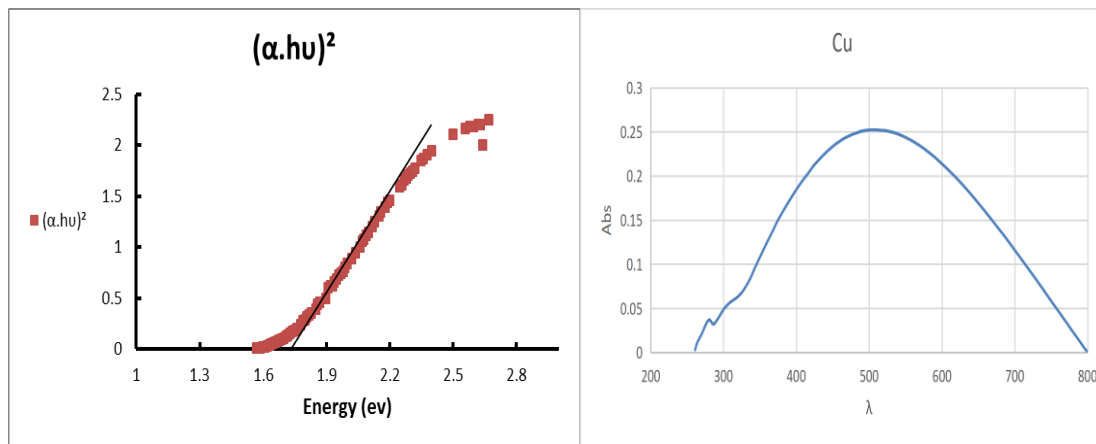


Fig.(5c) Electronic absorption spectrum of doped Cu-TiO₂ NP in nujol mull and Tauc plot of $(\alpha h\nu)^2$

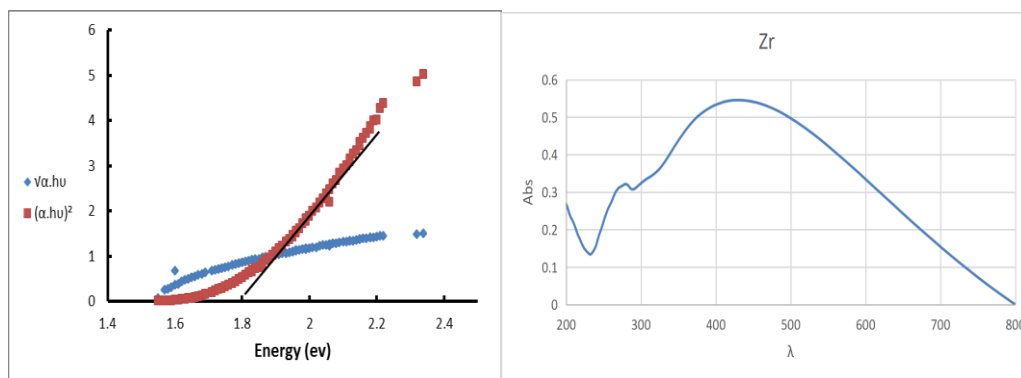


Fig.(5d) Electronic absorption spectrum of doped ZrO-TiO₂ NP in nujol mull and Tauc plot of $(\alpha h\nu)^2$

Conclusion

An efficient eco-friendly method for the preparation of TiO₂ NP was studied. To improve some physical properties of the as-prepared Nano particles, Fe, Cu, Zn and Zr were successfully doped In the TiO₂ NP. The chemical and physical structure of the prepared samples were characterized by different techniques. It was discovered that the doping

process improves the catalytic activity of TiO₂ NP by lowering its gap energy from 3.53 Ev in TiO₂ NP to 1.61, 1.65, and 1.8 ev for Fe, Cu, and Zr doped NP, respectively, allowing its use in the visible rather than the ultraviolet region of light. The main goal of the study is to examine the effect of the doping cation on the structural and photocatalytic properties of titanium dioxide.

References

- [1] A. Khlyustova, N. Sirotkin, T. Kusova, A. Kraev, V. Titov and A. Agafonov, "Doped TiO₂: the effect of doping elements on photocatalytic activity". *Mater. Adv.*, 1,(2020), 1193
- [2] W. Chakhari, J. Ben Naceur, S. Ben Taieb, I. Ben Assaker and R. Chtourou, "Fe-doped TiO₂ Nanorods with enhanced electrochemical properties as efficient photoanode materials", *J. Alloys & Comp.*, 708, (2017), 862-870,
- [3] S. S. Muniandy, N. H. M. Kaus, Z. T. Jiang, M. Altarawneh and H. L. Lee "Green synthesis of mesoporous anatase TiO₂ Nanoparticles and their photocatalytic activities", *RSC Adv.*, 7, (2017), 48083-48094.
- [4] N. Nasralla, M. Yeganeh, Y. Astuti, S. Piticharoenphun, N. Shahtahmasebi, A. Kompany, M. Karimipour, B.G. Mendis, N.R.J. Poolton, L. Šiller," Structural and spectroscopic study of Fe-doped TiO₂ Nanoparticles prepared by sol-gel method", *Scientia Iranica*, 20, (3), (2013), 1018-1022,
- [5] N. Nasralla, M. Yeganeh, Y. Astuti, S. Piticharoenphun, N. Shahtahmasebi, A. Kompany, M. Karimipour, B.G. Mendis, N.R.J. Poolton and L. Šiller," Structural and spectroscopic study of Fe-doped TiO₂ Nanoparticles prepared by sol-gel method", *Scientia Iranica*, 20, (3), (2013), 1018-1022,
- [6] D.T. Nguyen, S. S. Hong, "Synthesis of Metal Ion-Doped TiO₂ Nanoparticles Using Two-Phase Method and Their Photocatalytic Activity Under Visible Light Irradiation", *JNanosciNanotechnol.* 16(2) ,(2016),1911-5,doi: 10.1166/jnn.2016.11971. PMID: 27433699.
- [7] I. Ganesh I, A. K. Gupta, Kumar PP, Sekhar PS, Radha K, Padmanabham G, Sundararajan G. "Preparation and characterization of Ni-doped TiO₂ materials for photocurrent and photocatalytic applications", *Scie. World. J.* 2012;(2012):127326..
- [8] Ahmed M. Bolbol, Omar H. Abd-Elkader, Hassan Elshimy, Zaki I. Zaki, Salah A. Shata, M. Kamel, Ahmed S. Radwan, Nasser Y. Mostafa, " The effect of Zr (IV) doping on TiO₂ thin film structure and optical characteristics," *Results in Physics*, 42, (2022), 105955.
- [9] Prakash S. Pawar, Pramod A. Koyale, Vijay S. Ghodake, Swapnajit V. Mulik, Yash G. Kapdi, Saurabh S. Soni, Navaj B. Mullani, Sagar D. Delekar, "Design and photovoltaic studies of W@TiO₂ Nano composites with polymer gel electrolyte", *New J. Chem.* 47 (47), (2023), 21825-21833.
- [10] Rahimi HR, Arastoo M, Ostad SN, "A Comprehensive Review of Punica granatum (Pomegranate) Properties in Toxicological, Pharmacological", *Cell. & Mole. Biology Res.*, Iran J Pharm Res. 11(2) ,(2012);385-400.
- [11] B. Tryba*, M. Piszcz and A.W. Morawski; "Photocatalytic and Self-Cleaning Properties of Ag-Doped TiO₂" *The Open Materials Science Journal*, 2010, 4, 5-8 5 1874-088X/10 2010.
- [12] Reddy BM and Ganesh I. "Characterization of La₂O₃-TiO₂ and V₂O₅/La₂O₃-TiO₂ catalysts and their activity for synthesis of 2,6-dimethylphenol", *J. Mol. Cat. A.* 169(1-2), (2001); 207-223.
- [13] Tan Phat Chau, Geetha Royapuram Veeraragavan, Mathiyazhagan Narayanan, Arunachalam Chinnathambi, Sulaiman Ali Alharbi, Baskaran Subramani, Kathirvel Brindhadevi, Tipsukon Pimpimon, Surachai Pikulkaew," Green synthesis of Zirconium Nanoparticles using Punica granatum (pomegranate) peel extract and their antimicrobial and antioxidant potency," *Env. Res.* 209, (2022), 12771.
- [14] D. Ziental, B. Czarzynska-Goslinska, D.T. Mlynarczyk, A. Glowacka-Sobotta, B. Stanisz, T. Goslinski and L. Sobotta" Titanium Dioxide Nanoparticles: Prospects and Applications in Medicine", *Nanomaterials*, 10, (2020), 387; doi:10.3390/Nano10020387
- [15] Debandana Apta, Susanta Kumar Das, Maya Devi. Study of Variation in Optical Properties and Dispersion Parameters of Fe-Doped TiO₂ Nanopowders. *Transactions on Electrical and Electronic Materials*, 25 (1), 2024, 59-66.
- [16] Eleni Amyrgialaki, Dimitris P Makris, and Panagiotis Kefalas, "Optimisation of the extraction of pomegranate (Punica granatum) husk phenolics using water/ethanol solvent systems and response surface methodology" *Ind. Crops & Products* 59, (2014), 216-222.
- [17] Kumari S, Chaudhary YS and S. A. Agnihotry "A photoelectrochemical study of Nanostructured Cd-doped

- titanium oxide". *Inte. J. Hydrogen Energy*. 32(9), (2007); 1299–1302.
- [18] A. Ahmad, Lina A. Alakhras, Qais M. Al-Bataineh and A. Telfah, "Impact of metal doping on the physical characteristics of anatase titanium dioxide (TiO₂) films", *J Mater Sci: Mater Electron* (2023) 34:1552
- [19] I. M. I. Moustafa, D. N. Abdel Razek, Z.A. Omran and N.M. Mohamed; "Facile Preparation of Silver Halide Nanoparticles for Biological Application and Waste Water Treatment" *Advances in Nanoparticles*, 12, (2023), 123-138 ,
- [20] Raghvendra S. Dubey, Sandesh R. Jadkar, and Ajinkya B. Borde," Synthesis and Characterization of Various Doped TiO₂ Nanocrystals for Dye-Sensitized Solar Cells", *ACS Omega*,6 (5), (2021) , 3470-3482.
- [21] P. Scherrer, *Göttinger Nachrichten Gesell.*, 2, (1918), 98.
- [22] A. Patterson; "The Scherrer Formula for X-Ray Particle Size Determination", *Phys. Rev.*, 56 (10), (1939), 978–982.
- [23] Peverga R. Jubu and O.S. Obaseki and A. Nathan-Abutu and F.K. Yam and Yushamdan Yusof and M.B. Ochang;" Dispensability of the conventional Tauc's plot for accurate bandgap determination from UV–vis optical diffuse reflectance data" *Results in Optics*, 9, (2022), 100273.